

Dual Self-Healing Abilities of Composite Gels Consisting of Polymer-Brush-Afforded Particles and an Azobenzene-Doped Liquid Crystal

Yuki Kawata,^{†,‡} Takahiro Yamamoto,^{*,†} Hideyuki Kihara,[†] and Kohji Ohno^{*,§}

[†]Nanosystem Research Institute, National Institute of Advanced Industrial Science and Technology, 1-1-1 Higashi, Tsukuba, Ibaraki 305-8565, Japan

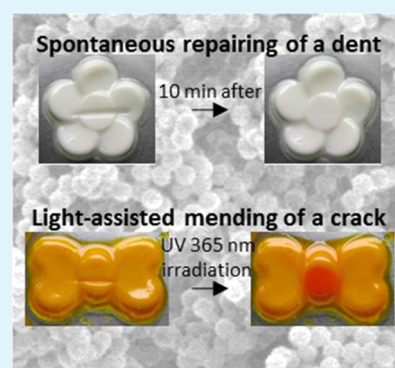
[‡]Department of Chemistry, Faculty of Pure and Applied Sciences, University of Tsukuba, 1-1-1 Tennodai, Tsukuba, Ibaraki 305-8571, Japan

[§]Institute for Chemical Research, Kyoto University, Gokasho Uji-City, Kyoto, 611-0011, Japan

Supporting Information

ABSTRACT: We prepared the composite gels from polymer-brush-afforded silica particles (P-SiPs) and an azobenzene-doped liquid crystal, and investigated their inner structure, dynamic viscoelastic properties, thermo- and photoresponsive properties, and self-healing behaviors. It was found that the composite gels had a sponge-like inner structure formed with P-SiPs and exhibited good elastic property and shape recoverability. The surface dents made on the composite gel could be repaired spontaneously at room temperature. Moreover, the composite gel exhibited a gel–sol transition induced by the *trans*–*cis* photoisomerization of the azo dye, and the transition could be used as a mending mechanism for surface cracks. Consequently, we successfully developed a material exhibiting two types of self-healing abilities simultaneously: (1) spontaneous repair of surface dents by means of the excellent elasticity of the composite gel and (2) light-assisted mending of surface cracks by photoinduced gel–sol transition.

KEYWORDS: liquid crystal, gel, azobenzene, self-healing, phase separation



1. INTRODUCTION

Over the past decade, self-healing materials have attracted a great deal of attention owing to their potential ability to extend the lifetime of products.^{1–3} So far, several materials that can heal cracks and cuts have been proposed on the basis of various approaches, such as utilization of encapsulated-polymerizable mobile phases to fill up cracked areas^{1–4} and dynamic covalent or noncovalent bonds that show recombination at the contact plane of cutting sections.^{3,5–9} In addition, morphological changes of materials such as a gel–sol transition would be potentially applicable to a healing mechanism of surface cracks.^{10–14} On the other hand, the repairing of surface dents was achieved using several polyurethanes and supramolecular materials.¹⁵ In addition, self-healing of internal delamination damages in fiber-reinforced composites by the microvascular delivery of reactive fluids was recently reported.¹⁶ An ideal self-healing material can heal various mechanical damage, such as cracks, cuts, dents, and delamination, made on/in a single material spontaneously or with the aid of external triggers such as light or heat. At present, materials that can thermally heal cuts and dents in a material have been realized with the use of hyperbranched polymers.¹⁷ However, the development of materials with multiple self-healing abilities is still a significant challenge.

Recently, gel materials using liquid crystals (LCs) as host matrices have been extensively studied as novel materials for

electro-optic applications.^{18–21} In our previous study, we have proposed an application of LC gels to self-healing materials and successfully demonstrated light-assisted mending of surface cracks by photochemical gel–sol transition of composite gels consisting of LCs, an azobenzene compound, and cross-linked polymer particles made from polystyrene and divinylbenzene.^{22,23} However, the composites had low mechanical strength and exhibited a rather plastic behavior. Therefore, unfortunately, surface dents made on the composite gels could not be repaired. In this study, we used the polymer-brush-afforded silica particle (P-SiP)²⁴ as a particle component of the composite gels to improve their elastic nature. The P-SiP is a core–shell particle in which the core is a monodisperse spherical silica particle and the shell consists of poly(methyl methacrylate) (PMMA) chains densely grafted on the core via an atom transfer radical polymerization (ATRP) method. A nematic LC material (4-pentyl-4'-cyanobiphenyl (5CB)) containing the P-SiP exhibited a self-supporting gel at room temperature. Subsequently, we investigated the structural properties, thermo- and photoresponsiveness, and dual self-healing abilities (spontaneous repairing of surface dents and

Received: December 1, 2014

Accepted: February 3, 2015

Published: February 3, 2015

light-assisted mending of surface cracks) of P-SiP/SCB composite gels containing an azobenzene compound.

2. EXPERIMENTAL SECTION

2.1. Materials. The P-SiP (Figure 1a) was synthesized by a surface-initiated ATRP of methyl methacrylate on spherical

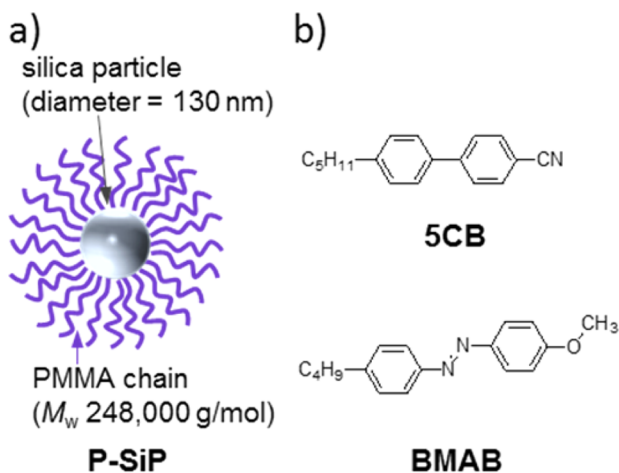


Figure 1. (a) Schematic illustration of a P-SiP and (b) chemical structures of liquid crystal (SCB) and an azobenzene compound (BMAB).

silica cores ($d = 130$ nm), as reported previously.²⁴ The molecular weight of the grafted PMMA chains was approximately $248\,000\text{ g mol}^{-1}$. The surface density of the grafted PMMA chains is typically $0.6\text{--}0.7\text{ chain/nm}^2$.²⁵ The diameter of the P-SiP was 650 nm, determined by dynamic light scattering measurements (Zetasizer Nano ZS, Malvern Instruments Ltd, UK) in acetone at $25\text{ }^\circ\text{C}$. The volume of a single P-SiP is roughly estimated as $(0.3\text{--}1.2) \times 10^{-12}\text{ cm}^3$ from scanning electron microscope and dynamic light scattering experiments. A nematic LC (4-pentyl-4'-cyanobiphenyl (SCB, Figure 1b) was purchased from Merck and used as supplied. The clearing temperature (T_C) of SCB was determined as $35\text{ }^\circ\text{C}$ by polarizing optical microscopy. An azobenzene compound (4-butyl-4'-methoxyazobenzene (BMAB, Figure 1b)²⁶ was prepared according to conventional synthetic routes and used as a photoresponsive additive.

2.2. Preparation of Composite Gels. A toluene dispersion of P-SiP and SCB was weighed in a glass vial, and toluene was evaporated under reduced pressure at $60\text{--}70\text{ }^\circ\text{C}$. The resulting composite was subsequently heated at $100\text{ }^\circ\text{C}$ and vigorously mixed, where the composite showed the sol state. The composite was then cooled to $25\text{ }^\circ\text{C}$ to induce gel formation. In the photoresponsive studies of the composite gels, we added an appropriate amount of BMAB to the P-SiP/SCB composite gels. In this study, the concentration of the P-SiP was adjusted to $10\text{ wt } \%$. Each composite gel was kept overnight at $25\text{ }^\circ\text{C}$ before each experiment was performed.

2.3. Scanning Electron Microscope (SEM) Observation. The P-SiP/SCB composite gel was soaked in hexane and dried repeatedly to remove SCB from the composite gel. The prepared xerogel was cut through and coated with 2 nm Pt-Pd particles. The cutting plane of the xerogel was observed on an SEM (S4300, Hitachi High-Technologies, Tokyo, Japan).

2.4. Optical Microscope Observation. The optical textures of the composite gels were observed using an optical

microscope (BX51, Olympus, Tokyo, Japan) with cross-polarized and phase-contrast modes.²⁷ The composite gels were put into the evaluation cells with its space of $30\text{ }\mu\text{m}$ and no surface coating. The temperature was controlled by a hot stage (FP80 + FP82, Mettler-Toledo, Tokyo, Japan). The textures were observed with and without the irradiation of a focused UV beam (wavelength = 365 nm , 1.6 mW/cm^2).

2.5. Dynamic Viscoelastic Properties. In a rheometer (MCR302, Anton-Paar Japan, Tokyo, Japan) with a parallel-plate type geometry (plate diameter = 12 mm), the composite gel placed between plates was heated to sol state and the gap between the plates was adjusted to an appropriate value. Next, the composite gel was cooled to room temperature and left for 1.5 h . Subsequently, the composite gel was heated to $34\text{ }^\circ\text{C}$, and the gap was readjusted to an appropriate value. The dynamic storage (G') and loss (G'') moduli of the P-SiP/SCB composite gel were measured at $25\text{ }^\circ\text{C}$ (strain = 0.1%). In the photoresponsive studies of the composite gels, we measured both moduli of P-SiP/BMAB/SCB composite gel (BMAB = $5\text{ mol } \%$) at $34\text{ }^\circ\text{C}$ (strain = 0.1% ; frequency = 1 Hz) with and without irradiation of UV light (wavelength = 365 nm , intensity = 180 mW/cm^2).

2.6. Spontaneous Repairing of Surface Dents. A digital force gauge (FGP-50, Nidec-shimpo, Kyoto, Japan) with a tool in slotted screwdriver form (the contact surface was $0.3\text{ mm} \times 10\text{ mm}$) was pressed onto the molded composite gels at $25\text{ }^\circ\text{C}$. After removing the mechanical stress, the repair process of the resulting surface dent was investigated at $25\text{ }^\circ\text{C}$ by visual observation.

2.7. Light-Assisted Mending of Surface Cracks. The cracked area made on P-SiP/BMAB/SCB composite gel was irradiated with a focused UV beam (wavelength = 365 nm , 8.5 mW/cm^2) at $30\text{ }^\circ\text{C}$. Then, the UV-irradiated gel was illuminated with visible light (wavelength = 450 nm , 40 mW/cm^2) at room temperature. The photochemical mending behavior was investigated by visual observation.

3. RESULTS AND DISCUSSION

3.1. Inner Structures and Viscoelastic Properties of P-SiP/SCB Composite Gel. First, we investigated the inner structures of the P-SiP/SCB composite gel using a scanning electron microscope (SEM). Figure 2a shows an SEM image of the cutting plane of a xerogel prepared from the P-SiP/SCB composite gel by removing the SCB. It can be seen that the P-SiP aggregates form a sponge-like structure that would contribute to the solid-like nature of the P-SiP/SCB composite. Interestingly, there was no significant shrinkage of the composite gel even after removing the SCB. Thus, a xerogel was successfully produced from the P-SiP/SCB composite gel, although a xerogel could not be prepared from the particle/LC composite gels in previous reports^{22,23} because of the collapse of particle assemblies caused by the removal of the LC matrices. The inner structures of the P-SiP/SCB composite gel were firmly supported by the interparticle entanglement of the PMMA chains of P-SiPs. The length of the grafted PMMA chains was long enough to form entanglement of the polymer chains (molecular weight of grafted PMMA chain was $248\,000\text{ g mol}^{-1}$).

The introduction of polymer chains onto the particle surface had a significant influence on the viscoelastic parameters of the particle/LC composite gels. The storage (G') and loss (G'') moduli of the P-SiP/SCB composite gel at $25\text{ }^\circ\text{C}$ were 4.6×10^4 and $5.2 \times 10^4\text{ Pa}$, respectively (strain = 0.1% ; frequency = 1

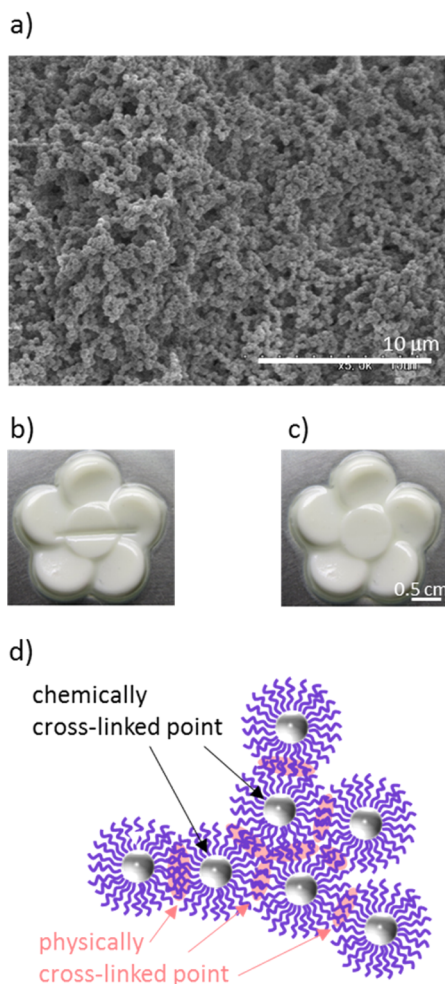


Figure 2. (a) SEM image of a xerogel prepared from P-SiP (10 wt %)/SCB composite gel. Photographs of P-SiP (10 wt %)/SCB composite gel at 25 °C taken (b) immediately after being pressed with a tool in slotted screwdriver form at 3 MPa and (c) 10 min after the press. (d) Schematic illustrations of a sponge-like structure formed in P-SiP/SCB composite gels.

Hz). The G' of the P-SiP/SCB composite gel (P-SiP concentration = 10 wt %) was ten times higher than that of particle/SCB composite gels (particle concentration = 28.6 wt %) previously reported,²² in which the previous particle had no chemically grafted polymer chains on its surface. The high G' of the P-SiP/SCB composite gel could be attributed to the reinforcement of the sponge-like structures formed with P-SiPs by the interparticle entanglement of PMMA chains.

3.2. Spontaneous Repairing of a Surface Dent. To examine one of self-healing abilities, that is, spontaneous repair of a surface dent, we performed mechanical stress tests with a tool in slotted screwdriver form (the contact area was 0.3 mm × 10 mm) at a given stress on the P-SiP/SCB composite gel at 25 °C. The composite gel was locally deformed by indentation at a pressure of 3 MPa with the tool, at which the gel was not broken (Figure 2b). Subsequently, after leaving the dented P-SiP/SCB composite gel for 10 min, the dent completely disappeared, indicating that the surface dent was repaired spontaneously (Figure 2c). Although there are variations in the breaking strength of the P-SiP/SCB composite gels depending on preparation conditions such as room temperature, none of the composite gels was broken by the indentation at pressures

below 1.5 MPa, and one of them could resist a pressure of up to 10 MPa (Supporting Information, Figure S1). If the composite gel was not broken by the indentation, every dent made on the gel disappeared spontaneously after removing the mechanical stress within several tens of minutes at 25 °C. On the other hand, when a previously reported particle/LC composite gel²² was subjected to an indentation, the composite gel was easily broken by the indentation at a pressure below 1 MPa (Supporting Information, Figure S2). The inferior mechanical properties of the previously reported composite gels were attributed to the brittle networks formed by weak physical interactions between particles, which had no grafted polymer chains on the surface. Thus, the composite gel could not deform without the collapse of the networks. Such phenomenon has often been observed in a physical gel. In contrast, as mentioned above, the P-SiP/SCB composite gels showed an elastic nature despite being a physical gel, which suggests that the network in the composite gel could be elastically deformed with mechanical stress and return to an original state after removing the stress.

It was previously reported that a nematic LC (7CB, 4-heptyl-4'-cyanobiphenyl) acted as a plasticizer in a PMMA/7CB blend system, and the glass transition temperature (T_g) of the blend was shifted from 105 to 40 °C as the 7CB concentration increased from 0 to 45 wt %.²⁷ We determined here the second virial coefficients of PMMA in isotropic LCs (5CB or 7CB) by static light scattering and roughly confirmed that PMMA had stronger affinity for 5CB compared to 7CB (see details in Supporting Information). Therefore, we inferred that 5CB would plasticize PMMA chains more efficiently. This implies that T_g of free PMMA/5CB blends should be lower than that of free PMMA/7CB blends. We believe that in the case of the P-SiP/5CB composite gel, PMMA chains in the composite gel would be plasticized by 5CB, so that the chains would show a rubbery nature even at room temperature. The flexible PMMA chains in the P-SiP/5CB composite gel would respond to mechanical stress by their conformational change, and entropically return to stable conformation after removing the stress. Furthermore, in the sponge-like structure formed with P-SiPs, we can consider that PMMA chains were cross-linked not only physically but also chemically (Figure 2d). The physical cross-linking points are interparticle entanglement points of PMMA chains. The chemical points are the silica cores of P-SiPs, on which one end of PMMA chains were chemically bonded. The chemical cross-linking points would regulate the spatial positions of the PMMA chains even if the physical cross-linking points slide by the application of the mechanical stress. Consequently, although the P-SiP/5CB composite gel was a physical gel as mentioned above, the sponge-like structures consisting of P-SiPs also behaved like a chemically cross-linked rubber network. Therefore, compared with the previously reported composite gels,²² the P-SiP/5CB composite gel showed high mechanical strength and efficient repair of surface dents. On the other hand, in the case of free PMMA/5CB blends, while they had high storage modulus similar to that of the P-SiP/5CB composite gel (Supporting Information, Figure S3), a surface dent on the free PMMA/5CB blend was not completely repaired within several tens of minutes (Supporting Information, Figure S4). The reason the free PMMA/5CB blend showed low elastic property against the indentation is considered as follows. The inner structure of the blend only had physical cross-linking points, that is, the entanglement points of PMMA chains. The mechanical indentation could cause

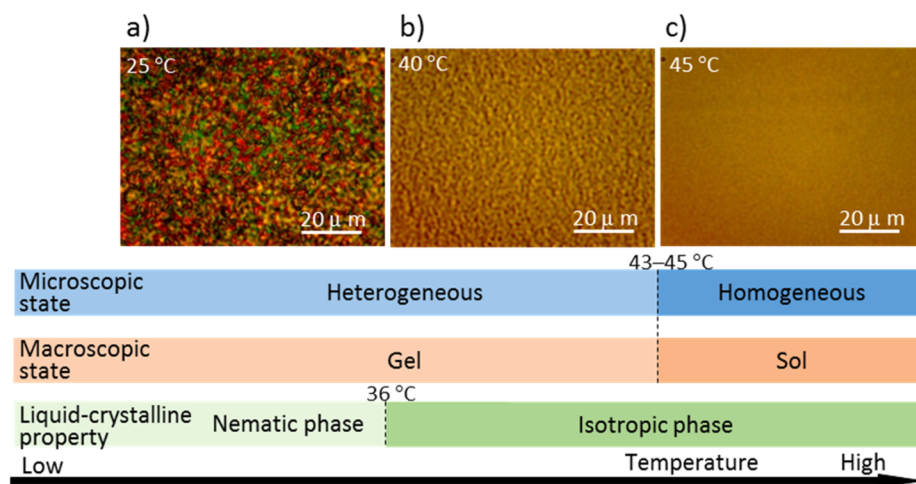


Figure 3. Thermal changes of microscopic and macroscopic states, and LC phases of P-SiP/SCB composite gels: (a–c) Optical micrographs of P-SiP/SCB composite gel (P-SiP = 10 wt %) at each temperature (upper part); (a) in cross-polarized mode; (b,c) in phase-contrast mode. Morphology changes in the composite gel are shown in lower parts.

positional changes in the PMMA chains as well as the slide of the entanglement points. Therefore, shape recovery of the PMMA/SCB blend did not occur efficiently. The efficiency of the spontaneous repair and the mechanical strength of the composite gels will be greatly affected by the molecular weight of the grafted PMMA chains and the particle concentration in the composite gels. We tentatively found that the composite gels exhibit poor viscoelastic and healing properties when the molecular weight of the grafted PMMA chains was lower than approximately 20 000. In addition, we have roughly estimated that the minimum particle concentration required to obtain self-supporting gels is approximately 5 wt %. Further studies on the effects of the molecular weight of the polymer and the concentration of P-SiP on the breaking strength and shape recoverability of the P-SiP/SCB composite gels are in progress.

3.3. Thermal Properties and Gelation Mechanism of the Composite Gels. Next, we investigated the thermal properties of P-SiP/SCB composite gel (Figure 3). Macroscopically, a P-SiP/SCB composite was in the gel state at room temperature, and was transformed into the sol state after heating. The gel–sol transition temperature (T_{GS}) was estimated to be 43–45 °C. Subsequently, we investigated the liquid-crystalline properties and microscopic morphologies of the P-SiP/SCB composites by optical microscope observation in crossed-polarized and phase-contrast modes. According to the previous report,²⁷ even if the difference in the refractive indices between polymer and isotropic LC is not so large, the phase separation between the two materials is clearly observed in phase-contrast mode equipped with polarizer only. Therefore, in this study, nematic–isotropic phase transition of SCB and phase separation between P-SiP and nematic SCB can be investigated by the crossed-polarized mode. In addition, the phase-separated state between P-SiP and isotropic SCB can be distinguishable by means of the phase-contrast mode. The P-SiP/SCB composite gel exhibited the nematic–isotropic phase transition at 36 °C, which was almost identical to the clearing temperature (T_C) of pure SCB. However, a heterogeneous microstructure, which would originate from a phase separation between P-SiP-rich and SCB-rich phases, was observed until 45 °C, which coincided with the T_{GS} . Therefore, we consider that the gel state resulted from the formation of the heterogeneous microstructure, which would correspond to a sponge-like

structure shown in Figure 2a. In a series of previous studies of particle/LC composite gels, the gelation of LCs has been generally explained by the formation of particle networks by the expulsion of particles from LC domains on the isotropic–LC phase transition.^{28,29} Consequently, the T_{GS} of composite gels coincided with the T_C of LCs. However, in this study, the T_{GS} of a P-SiP/SCB composite gel was higher than the T_C of SCB as mentioned above. This result indicates that the gel state and the heterogeneous microstructure were observed even in the isotropic phase of SCB. Similar to a previous report by Bukusoglu and co-workers,³⁰ the phase separation between particles and isotropic LC matrix was expected to also be triggered by the thermodynamic instability of the composite system consisting of P-SiP and isotropic SCB. We presumed that the interaction between the PMMA shell of P-SiP and isotropic SCB would affect the thermodynamic instability. Actually, we estimated that the upper critical solution temperature of PMMA was approximately 40 °C in SCB (Supporting Information, Figure S5), which was close to the T_{GS} (43–45 °C) of the P-SiP/SCB composite gel. Of course, the thermal gel–sol transition and the transformation between heterogeneous and homogeneous structures were reversible. In a cooling process, the sol–gel transition and appearance of heterogeneous microstructures were observed at almost the same temperature as the heating process.

3.4. Photoresponsive Properties of Azo-Doped Composite Gels. Subsequently, we investigated the photoresponsive properties of P-SiP/SCB composite gels doped with an azobenzene compound (4-butyl-4'-methoxyazobenzene, BMAB) by polarized optical microscopy and rheological measurements. The phase structures of LCs can easily be modulated by *trans*–*cis* photoisomerization of azobenzene compounds added to LCs as dopants.³¹ In this study, if the nematic–isotropic phase transition was induced in a P-SiP/SCB composite gel by the photochemical manner, the contribution of nematic molecular ordering to free energy of a P-SiP/SCB mixture would change significantly. In that case, the photoinduced change of thermodynamic balance is expected to induce the transformation between the heterogeneous (gel) and homogeneous (sol) states of a P-SiP/SCB composite gel. Figure 4 shows the T_C and the disappearance temperatures of heterogeneous structures, which coincided

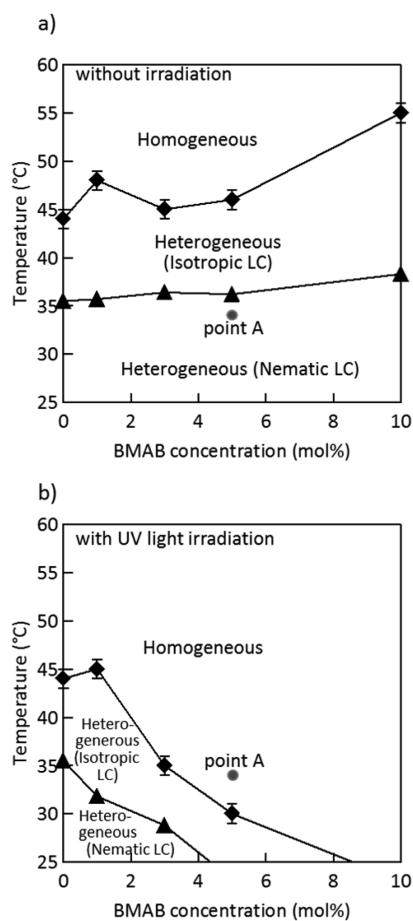


Figure 4. Phase diagrams of P-SiP/BMAB/SCB composite gel (P-SiP = 10 wt %) as a function of the concentration of BMAB (a) without and (b) with irradiation of UV light (wavelength = 365 nm, intensity = 1.6 mW/cm²). The heterogeneous–homogeneous transition (◆) and nematic–isotropic phase-transition (▲) temperatures were determined by optical microscopic observations of the composite gels in a heating process at a rate of 1 °C/min. At point A, gel–sol transition can be induced by irradiation of UV light.

with the T_{GS} , with and without the irradiation of UV light (wavelength = 365 nm, intensity = 1.6 mW/cm²). The temperatures were determined by microscopic observation of P-SiP/BMAB/SCB composite gels (BMAB = 0–10 mol % for SCB). Both temperatures of the azo-doped composite gels were significantly reduced by the photoirradiation, which induced the *trans*–*cis* photoisomerization. Here, at point A in Figure 4a,b, we expect that the photoirradiation induces a transition from the heterogeneous (gel) state to a homogeneous (sol) one of the P-SiP/BMAB/SCB composite. Figure 5 shows the changes in the optical textures and the viscoelastic property of the P-SiP/BMAB/SCB composite gel (BMAB = 5 mol % for SCB) with irradiation of the focused UV beam (intensity = 0.05 mW) at 34 °C (the experimental condition corresponded to point A in Figure 4). In the cross-polarized mode (Figure 5a), we observed that an optical texture in and around the irradiated area changed into the dark state by the generation and diffusion of the *cis* form of BMAB. This indicates that *trans*–*cis* photoisomerization of BMAB caused the isothermal nematic–isotropic phase transition of the LC matrix.³¹ With the photoirradiation, we also found that the heterogeneous microstructure in the irradiated area slowly disappeared for several minutes in the phase-contrast mode (Figure 5b). Thus,

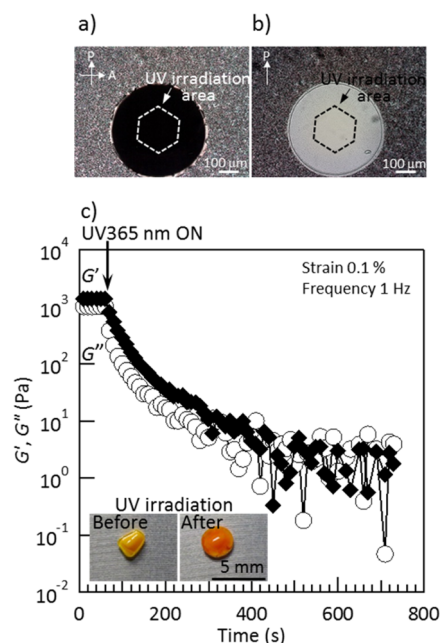


Figure 5. Photoinduced change in the microscopic structure and viscoelastic property of a P-SiP/BMAB/SCB composite gel (P-SiP = 10 wt %, BMAB = 5 mol % for SCB). Optical textures of the composite gel at 34 °C during irradiation of focused UV light (wavelength = 365 nm, intensity = 0.05 mW) were obtained in (a) cross-polarized and (b) phase-contrast modes. (c) Dynamic storage (G' , ◆) and loss moduli (G'' , ○) at a strain of 0.1%, frequency of 1 Hz, and temperature of 34 °C were measured with irradiation of UV light (wavelength = 365 nm, intensity = 180 mW/cm²). Inset photographs in (c) are the P-SiP/BMAB/SCB composite gels before and after irradiation with UV light.

the *trans*–*cis* photoisomerization induced changes not only in the phase structures of the LC matrix, but also in the microscopic morphologies of the composite gel. Figure 5c shows the rheology of the P-SiP/BMAB/SCB composite gel (BMAB = 5 mol % for SCB) under irradiation with UV light. The initial G' of the P-SiP/BMAB/SCB composite gel was over 10³ Pa at 34 °C. With the irradiation of the UV light (intensity = 180 mW/cm²), G' slowly decreased and became 10 Pa or less after 300 s. From macroscopic observations (inset of Figure 5c), we confirmed that the composite showed a liquid-like nature after photoirradiation. As we expected in Figure 4, the gel–sol transition of a P-SiP/SCB composite gel could be successfully induced by means of the *trans*–*cis* photoisomerization. The liquid-like P-SiP/BMAB/SCB composite induced by UV light irradiation reverted back to the solid-like composite after irradiation with visible light (wavelength = 450 nm, intensity = 40 mW/cm²) and then leaving it at room temperature without irradiation for 1 h (Supporting Information, Table S1). The G' values of the composite gel before UV light irradiation and after visible light irradiation were 3.1×10^4 and 2.0×10^4 Pa, respectively (strain = 0.1%; frequency = 1 Hz; temperature = 20 °C).

3.5. Dual Self-Healing Abilities of the Azo-Doped Composite Gel. Finally, we demonstrated here the dual self-healing abilities of the P-SiP/BMAB/SCB composite gel using the improved elastic nature and the photoinduced gel–sol transition of the composite gel (Figure 6). Mechanical stress (pressure = 3 MPa) was applied on the surface of the P-SiP/BMAB/SCB composite gel (BMAB = 10 mol % for SCB) with

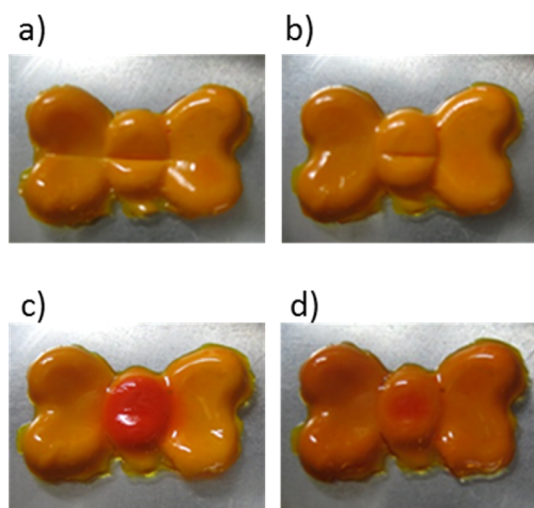


Figure 6. Photographs of a P-SiP/BMAB/SCB composite gel (P-SiP = 10 wt %, BMAB = 10 mol % for SCB): (a) immediately after being pressed with a tool in slotted screwdriver form at 3 MPa and 30 °C; (b) 10 min after the press; (c) after irradiation of a cracked area with focused UV light (wavelength = 365 nm, intensity = 8.5 mW/cm²) for 20 min at 30 °C; (d) after illumination of the UV-irradiated area with visible light (wavelength = 450 nm, intensity = 40 mW/cm²) for 20 min at 25 °C.

the tool mentioned earlier. With this external stress, a crack and a dent were produced at the central part and the left edge of the surface of the composite gel, respectively (Figure 6a). The surface dent spontaneously disappeared when the composite gel was left for 10 min at 25 °C, while the cracked area did not show any healing events (Figure 6b). Subsequently, we irradiated the cracked area with a focused UV beam (intensity = 8.5 mW/cm²) at 30 °C. The irradiated area of the composite gel attained the sol state and the surface crack was filled up with the composite in the sol state (Figure 6c). Subsequently, the UV light-induced sol area was illuminated with visible light (intensity = 40 mW/cm²) to induce sol–gel transition, resulting in the recovery of a smooth surface of the composite gel (Figure 6d).

The self-healing characteristics discussed in this study will be strongly dependent on various factors. For example, in the case of the spontaneous repair of surface dents, T_g of the grafted polymer will affect the efficiency of the repair of dents because the polymer chains need to act like rubbery chains. Then, it is preferred that T_g of the grafted polymer is lower than room temperature. In this study, the P-SiP/SCB composite gel successfully exhibits efficient repair of surface dents around room temperature, because the grafted PMMA chain would show a rubbery nature even at room temperature by plasticizing by SCB. In the case of the photochemical mending of surface cracks, gel–sol (heterogeneous–homogeneous) transition triggered by *trans–cis* photoisomerization of the doped azobenzene compound is required. The operating temperature range of the photochemical mending can be tuned by the concentration of the doped azobenzene compound as shown in Figure 4. With increasing concentration of the azo-dopant, the photochemical mending can be achieved at lower temperature.

4. CONCLUSIONS

In this study, we investigated the morphologies and self-healing abilities of particle/LC composite gels using P-SiP as a particle

component. The P-SiP/SCB composite gel was found to be a self-supporting gel. The SEM image of the xerogel exhibited that sponge-like aggregation structures of the P-SiPs were formed in the composite gels. The P-SiP/SCB composite gel showed high strength against mechanical stress and good shape recoverability. These mechanical properties of the composite gels could be attributed to a combination of the rubbery nature of PMMA chains plasticized with SCB in the shells of P-SiP and the regulatory effect of the spatial positions of PMMA chains chemically grafted on the particle core. In addition, the composite gels doped with an azobenzene compound exhibited gel–sol transition by the *trans–cis* photoisomerization of the dopant. The P-SiP/azo-doped SCB composite gel exhibited its dual self-healing abilities via the spontaneous repair of a surface dent and the light-assisted mending of a surface crack in a material.

■ ASSOCIATED CONTENT

Supporting Information

The mechanical stress tests (Figures S1, S2, and S4), the fundamental data of rheology (Figure S3), the upper critical solution temperature of PMMA/SCB solution (Figure S5), rheological data in light-assisted mending process (Table S1), and the affinity of PMMA and LCs. This material is available free of charge via the Internet at <http://pubs.acs.org>.

■ AUTHOR INFORMATION

Corresponding Authors

*E-mail: takahiro.yamamoto@aist.go.jp.

*E-mail: ohno@scl.kyoto-u.ac.jp.

Notes

The authors declare no competing financial interest.

■ ACKNOWLEDGMENTS

The authors acknowledge Dr. M. Masuda and Ms. M. Wada (AIST) for dynamic light scattering measurements. The authors greatly appreciate helpful comments and suggestions of Dr. J. Fukuda (AIST). This work was partly supported by JSPS KAKENHI Grant Number 25410217.

■ REFERENCES

- (1) Murphy, E. B.; Wudl, F. The World of Smart Healable Materials. *Prog. Polym. Sci.* **2010**, *35*, 223–251.
- (2) Hager, M. D.; Greil, P.; Leyens, C.; van der Zwaag, S.; Schubert, U. S. Self-Healing Materials. *Adv. Mater.* **2010**, *22*, 5424–5430.
- (3) Bergman, S. D.; Wudl, F. Mendable Polymers. *J. Mater. Chem.* **2008**, *18*, 41–62.
- (4) White, S. R.; Sottos, N. R.; Geubelle, P. H.; Moore, J. S.; Kessler, M. R.; Sriram, S. R.; Brown, E. N.; Viswanathan, S. Autonomic Healing of Polymer Composites. *Nature* **2001**, *409*, 794–797.
- (5) Liu, K.; Kang, Y.; Wang, Z.; Zhang, X. 25th Anniversary Article: Reversible and Adaptive Functional Supramolecular Materials: "Non-covalent Interaction" Matters. *Adv. Mater.* **2013**, *25*, 5530–5548.
- (6) Ying, H.; Zhang, Y.; Cheng, J. Dynamic Urea Bond for the Design of Reversible and Self-Healing Polymers. *Nat. Commun.* **2014**, *5*, 3218.
- (7) Zhang, H. J.; Xia, H. S.; Zhao, Y. Poly(vinyl alcohol) Hydrogel Can Autonomously Self-Heal. *ACS Macro Lett.* **2012**, *1*, 1233–1236.
- (8) Cordier, P.; Tournilhac, F.; Soulie-Ziakovic, C.; Leibler, L. Self-Healing and Thermoreversible Rubber from Supramolecular Assembly. *Nature* **2008**, *451*, 977–980.
- (9) Yamaguchi, H.; Kobayashi, Y.; Kobayashi, R.; Takashima, Y.; Hashidzume, A.; Harada, A. Photoswitchable Gel Assembly Based on Molecular Recognition. *Nat. Commun.* **2012**, *3*, 603.

- (10) Yang, R. M.; Peng, S. H.; Wan, W. B.; Hughes, T. C. Azobenzene Based Multistimuli Responsive Supramolecular Hydrogels. *J. Mater. Chem. C* **2014**, *2*, 9122–9131.
- (11) Ogawa, Y.; Yoshiyama, C.; Kitaoka, T. Helical Assembly of Azobenzene-Conjugated Carbohydrate Hydrogelators with Specific Affinity for Lectins. *Langmuir* **2012**, *28*, 4404–4412.
- (12) Tiefenbacher, K.; Dube, H.; Ajami, D.; Rebek, J. A Transparent Photo-Responsive Organogel Based on a Glycoluril Supergelator. *Chem. Commun. (Cambridge, U. K.)* **2011**, *47*, 7341–7343.
- (13) Matsuzawa, Y.; Tamaoki, N. Photoisomerization of Azobenzene Units Controls the Reversible Dispersion and Reorganization of Fibrous Self-Assembled Systems. *J. Phys. Chem. B* **2010**, *114*, 1586–1590.
- (14) Deindorfer, P.; Eremin, A.; Stannarius, R.; Davis, R.; Zentel, R. Gelation of Smectic Liquid Crystal Phases with Photosensitive Gel Forming Agents. *Soft Matter* **2006**, *2*, 693–698.
- (15) Noda, Y.; Hayashi, Y.; Ito, K. From Topological Gels to Slide-Ring Materials. *J. Appl. Polym. Sci.* **2014**, *131*, 40509.
- (16) Patrick, J. F.; Hart, K. R.; Krull, B. P.; Diesendruck, C. E.; Moore, J. S.; White, S. R.; Sottos, N. R. Continuous Self-Healing Life Cycle in Vascularized Structural Composites. *Adv. Mater.* **2014**, *26*, 4302–4308.
- (17) Wei, Q.; Wang, J.; Shen, X. Y.; Zhang, X. A.; Sun, J. Z.; Qin, A. J.; Tang, B. Z. Self-Healing Hyperbranched Poly(aryltriazole)s. *Sci. Rep.* **2013**, *3*, 1093.
- (18) Kato, T.; Hirai, Y.; Nakaso, S.; Moriyama, M. Liquid-Crystalline Physical Gels. *Chem. Soc. Rev.* **2007**, *36*, 1857–1867.
- (19) Chen, J. W.; Huang, C. C.; Chao, C. Y. Supramolecular Liquid-Crystal Gels Formed by Polyfluorene-Based π -Conjugated Polymer for Switchable Anisotropic Scattering Device. *ACS Appl. Mater. Interfaces* **2014**, *6*, 6757–6764.
- (20) Bobrovsky, A.; Shibaev, V.; Hamplova, V.; Kaspar, M.; Glogarova, M. Gel Formation and Photoactive Properties of Azobenzene-Containing Polymer in Liquid Crystal Mixture. *Colloid Polym. Sci.* **2010**, *288*, 1375–1384.
- (21) Nair, G. G.; Prasad, S. K.; Jayalakshmi, V.; Shanker, G.; Yelamaggad, C. V. Fast Responding Robust Nematic Liquid Crystalline Gels Formed by a Monodisperse Dipeptide: Electro-Optic and Rheological Studies. *J. Phys. Chem. B* **2009**, *113*, 6647–6651.
- (22) Yamamoto, T.; Yoshida, M. Viscoelastic and Photoresponsive Properties of Microparticle/Liquid-Crystal Composite Gels: Tunable Mechanical Strength along with Rapid-Recovery Nature and Photochemical Surface Healing using an Azobenzene Dopant. *Langmuir* **2012**, *28*, 8463–8469.
- (23) Yamamoto, T.; Kawata, Y.; Yoshida, M. Contrasting Roles of Layered Structures in the Molecular Assembly of Liquid Crystal Matrices on the Viscoelastic Properties of Microparticle/Liquid Crystal Composite Gels Leading to Rigidification and Destabilization. *J. Colloid Interface Sci.* **2013**, *397*, 131–136.
- (24) Ohno, K.; Morinaga, T.; Takeno, S.; Tsujii, Y.; Fukuda, T. Suspensions of Silica Particles Grafted with Concentrated Polymer Brush: A New Family of Colloidal Crystals. *Macromolecules* **2006**, *39*, 1245–1249.
- (25) Ohno, K.; Morinaga, T.; Takeno, S.; Tsujii, Y.; Fukuda, T. Suspensions of Silica Particles Grafted with Concentrated Polymer Brush: Effects of Graft Chain Length on Brush Layer Thickness and Colloidal Crystallization. *Macromolecules* **2007**, *40*, 9143–9150.
- (26) Tazuke, S.; Kurihara, S.; Ikeda, T. Amplified Image Recording in Liquid-Crystal Media by Means of Photochemically Triggered Phase-Transition. *Chem. Lett.* **1987**, *16*, 911–914.
- (27) Ahn, W.; Kim, C. Y.; Kim, H.; Kim, S. C. Phase-Behavior of Polymer Liquid-Crystal Blends. *Macromolecules* **1992**, *25*, 5002–5007.
- (28) Meeker, S. P.; Poon, W. C. K.; Crain, J.; Terentjev, E. M. Colloid-Liquid-Crystal Composites: An Unusual Soft Solid. *Phys. Rev. E* **2000**, *61*, R6083–R6086.
- (29) Vollmer, D.; Hinze, G.; Ullrich, B.; Poon, W. C. K.; Cates, M. E.; Schofield, A. B. Formation of Self-Supporting Reversible Cellular Networks in Suspensions of Colloids and Liquid Crystals. *Langmuir* **2005**, *21*, 4921–4930.
- (30) Bukusoglu, E.; Pal, S. K.; de Pablo, J. J.; Abbott, N. L. Colloid-in-Liquid Crystal Gels Formed via Spinodal Decomposition. *Soft Matter* **2014**, *10*, 1602–1610.
- (31) Ikeda, T. Photomodulation of Liquid Crystal Orientations for Photonic Applications. *J. Mater. Chem.* **2003**, *13*, 2037–2057.